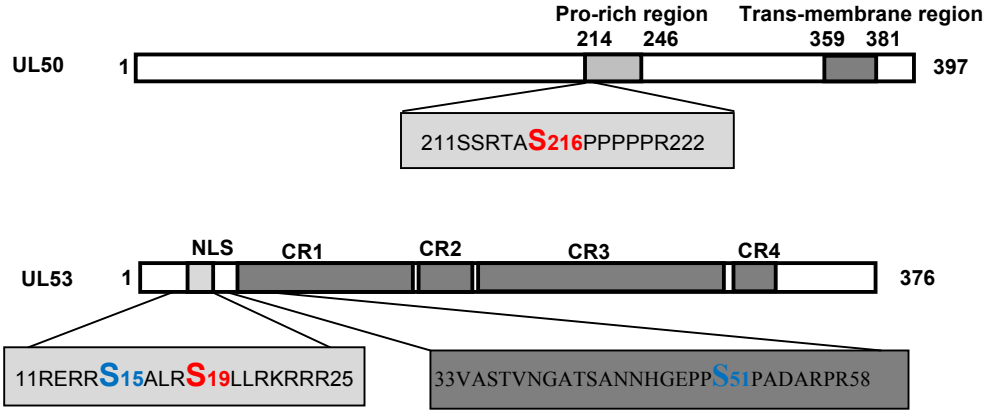

FIG S1. UL97 phosphorylation sites on the HCMV NEC. Schematic of HCMV UL50 and UL53 proteins highlighting the residues that were detected in mass spectrometric analyses of lysates from HCMV-infected HFF cells. The residues phosphorylated in a MBV-sensitive manner are highlighted in red; and the residues phosphorylated in the absence or presence of MBV are shown in blue (refer to Table 2). The schematic shows that UL50 residue Ser-216 is a part of the Pro-rich region of the protein critical for virus viability, and UL53 residue Ser-19 is a part of the nuclear localization sequence (NLS), located at amino acids 18-27. The four conserved regions (CR1-CR4), based on multiple sequence alignment, in HCMV UL53 are also indicated: CR1, residues 58 to 125; CR2, 127 to 160; CR3, 163 to 243; and CR4, 254 to 282.

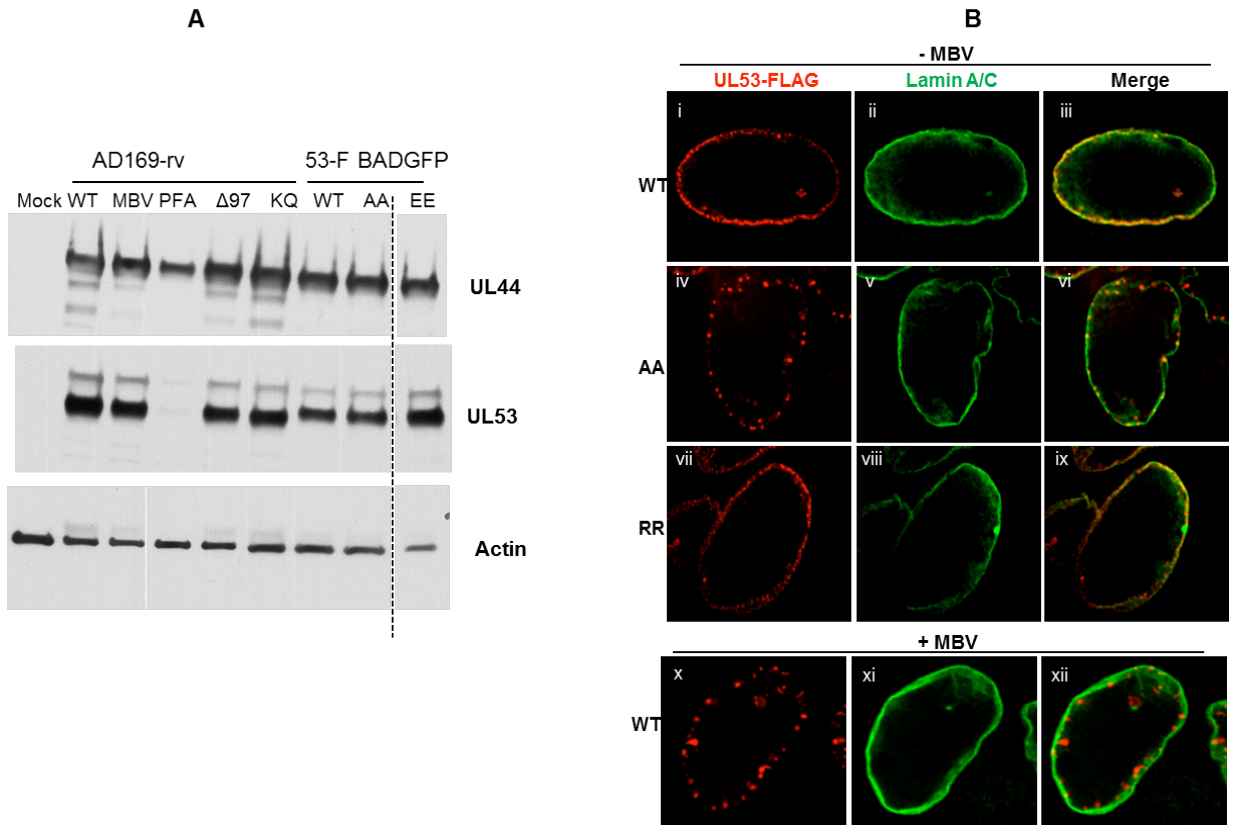

FIG S2**.** A. Maribavir, *UL97* mutations, and UL50-53 phosphorylation site substitutions do not meaningfully affect expression of UL53. HFF cells were mock-infected or infected with WT AD169-RV in the absence (WT) or presence of 1μM MBV or 520 μM phosphonoformic acid (PFA); or with a *UL97* null mutant (Δ97), a mutant carrying the kinase inactivating mutation K355Q (KQ), or with WT, AA, or EE 53-F BADGFP in the absence of inhibitors at an MOI of 1. At 72 h.p.i., lysates were obtained, proteins were separated by SDS-PAGE and immunoblotted, and probed with antibodies against the viral processivity factor, UL44, UL53, and the loading control, actin. B. Effect of UL50-53 phosphorylation site substitutions and maribavir on the localization of lamin A/C and the viral NEC at the nuclear rim. HFF cells were infected with WT 53-F BADGFP, or the double mutant, AA, or its rescued derivative, RR, at an MOI of 1, in the presence or absence of 1μM MBV (+ or – MBV). At 72 h.p.i., cells were fixed and stained for FLAG (red) and lamin A/C (green).

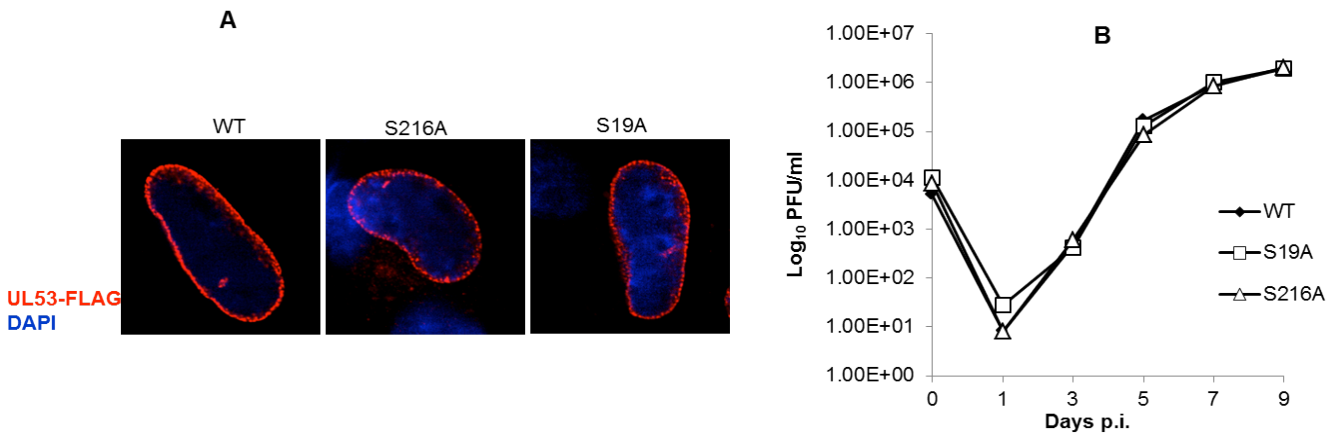

FIG S3. Effect of UL97 phosphorylation site substitutions in UL50 or UL53 on NEC localization and virus replication. A. HFF cells were infected with UL53-FLAG AD169-RV (53-F, designated as WT in the figure), or the 53-F virus carrying the single amino acid substitutions UL50 S216A, or UL53 S19A at an MOI of 1. At 72 h.p.i., cells were fixed and stained for FLAG (red) and the nucleus was stained with DAPI (blue). B. HFF cells were infected with either WT or mutant viruses carrying alanine substitutions of either UL50 residue S216 (S216A) or UL53 residue S19 (S19A), at an MOI of 0.1. At the indicated time points, supernatants were collected and titrated by plaque assay for infectious virus.

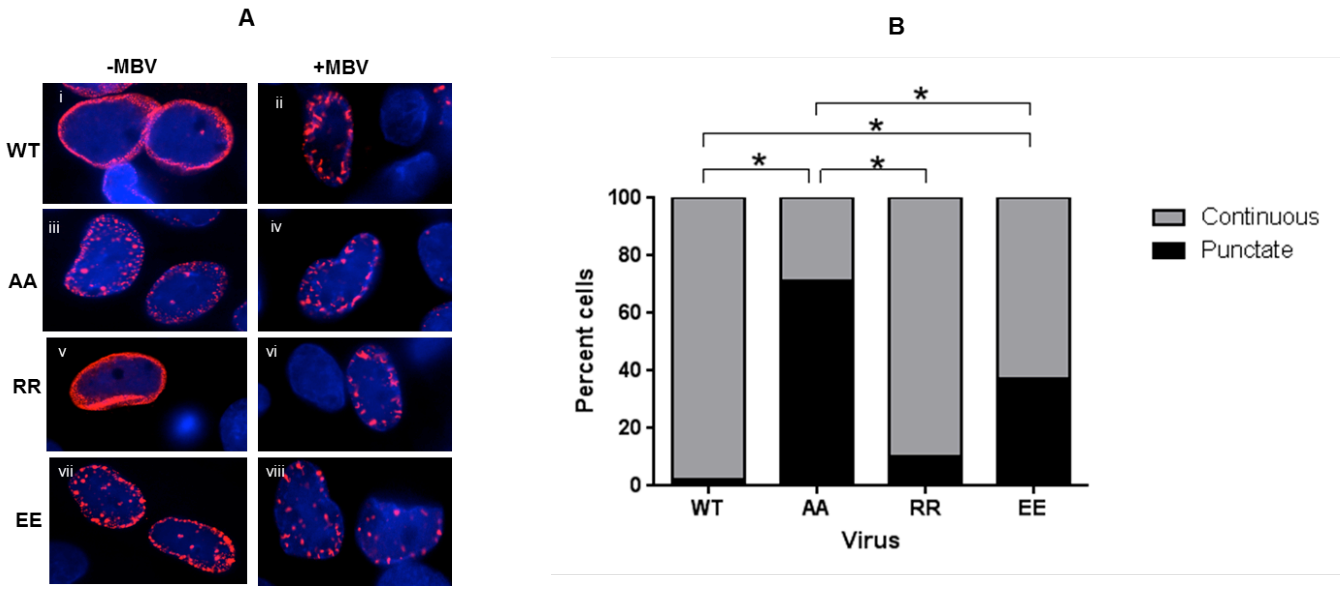

FIG S4. Color version of Fig. 5A. Effects of NEC substitutions on NEC distribution. A. HFF cells were infected with WT, AA, RR, or EE 53-F BADGFP (MOI=1), in the absence or presence of 1μM MBV. At 72 h.p.i. cells were fixed and stained with FLAG (red) and the nucleus was stained with DAPI (blue). B. Infected cells (n=42-102) were assessed for whether they showed any punctate staining for UL53-FLAG at the nuclear rim (black bars), or a continuous distribution at the nuclear rim (gray bars) in the absence of MBV. The differences between the data were analyzed using Fisher's exact test. * indicates $p<0.0001$. No label means no significant difference. For a family-wise type I error rate of 0.05 for each set of 5 comparisons, a result can only be considered significant when $p<0.0102$.

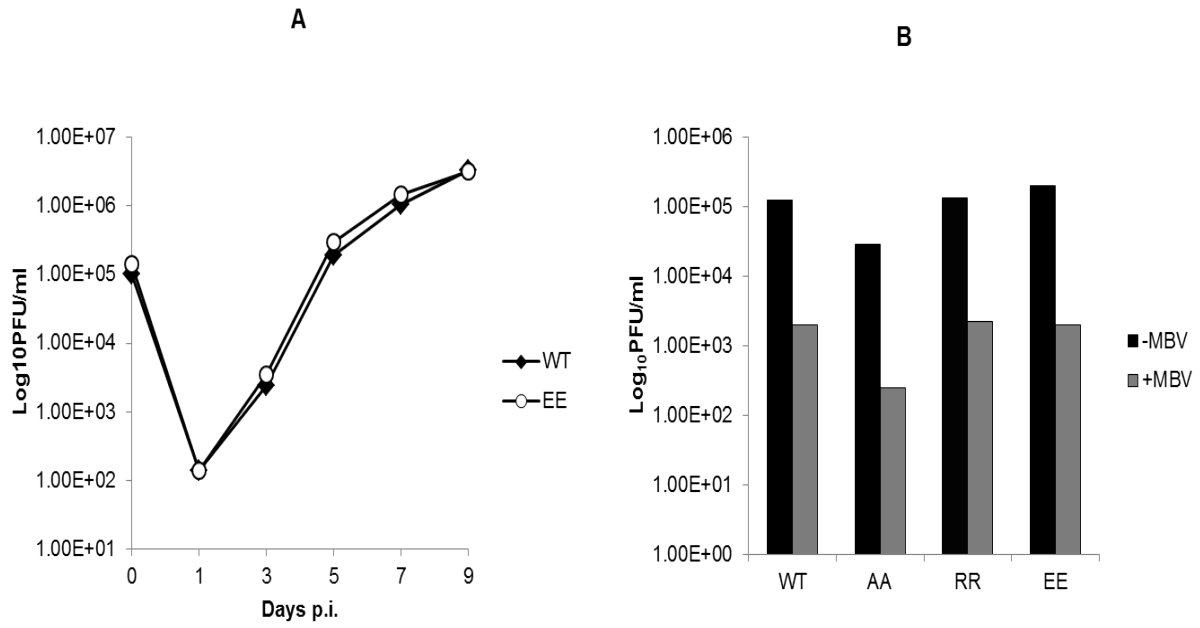

Fig S5. Effect of glutamate substitutions in UL50 and UL53 on virus replication. A. HFF cells were infected with either 53-F BADGFP (WT) or a mutant virus (EE) carrying glutamic acid substitutions of both UL50 residue S216 (S216E) and UL53 residue S19 (S19E), at an MOI of 0.1. At the indicated time points, supernatants were collected and titrated for infectious virus by plaque assay. Titers were calculated by averaging plaque counts from triplicate titrations. Because counts from three sets of titrations differed less than twofold for all data points, error bars are not shown. B. HFF cells were infected with WT, AA, RR, or EE 53-F BADGFP, at an MOI of 0.1, in the absence or presence of 1μM MBV. At day 5 p.i., supernatants were collected and titrated for infectious virus by plaque assay. Titers were calculated by averaging plaque counts from duplicate titrations. Because counts from two sets of titrations differed less than twofold for all data points, error bars are not shown.

Supplemental Table S1. Primer sequences for HCMV AD169 BAC or BADGFP constructs

Construct	Primer	Sequence
WT LMN-ΔH/C	97p-GFP-fw	AGCTAGTGCAGCCTTAGGAACAGGGAAGACTGTCGCCACTATGGTGAG CAAGGGCGAGG
	SV40_CAAX rv	TGTCTGCTCGAAGCGGCCGGCCGCCCCGACTCTAGAATTATTAGTTCT GGGGGCTCTGGGT
Δ97 LMN-ΔH/C	97subGFP_Fw	AGCTAGTGCAGCCTTAGGAACAGGGAAGACTGTCGCCACTATGGTGAG CAAGGGCGAGG
	97subCAAX_Rv (dCAAX)	TTGCCTTTCCCCTCAGCAACCGTCACGTTCCGCGTCCCGGTTAGTTCTG GGGGCTCTGGGT
S19A	S19A Fw	CGTGCGCACGCCGCGCGAACGACGCTCGGCCTTGCGCGCACTGCTCC GCAAGCGCCGCCATAGGGATAACAGGGTAATCG
	S19A Rv	GCTGGCCAGCTCGCGTTGGCGGCGCTTGCGGAGCAGTGCGCGCAAG GCCGAGCGTCGTTCGCCAGTGTTACAACCAATTAACC
S216A	S216A Fw	TACGCGAACGGCGGGAAAGCGGTCCTCTCGGACCGCAGCACCCCCTC CTCCTCCTCGTCATAGGGATAACAGGGTAATCG
	S216A Rv	GGTGGGAGAGCAACTCGGATGACGAGGAGGAGGAGGGGGTGCTGCG GTCCGAGAGGACCGGCCAGTGTTACAACCAATTAAC
S19AR-S216AR (RR)	S19A Res Fw	CGTGCGCACGCCGCGCGAACGACGCTCGGCCTTGCGCTCCCTGCTCC GCAAGCGCCGCCATAGGGATAACAGGGTAATCG
	S19A Res Rv	GCTGGCCAGCTCGCGTTGGCGGCGCTTGCGGAGCAGGGAGCGCAAG GCCGAGCGTCGTTCGCCAGTGTTACAACCAATTAACC
	S216A Res Fw	TACGCGAACGGCGGGAAAGCGGTCCTCTCGGACCGCATCTCCCCCTC CTCCTCCTCGTCATAGGGATAACAGGGTAATCG
	S216A Res Rv	GGTGGGAGAGCAACTCGGATGACGAGGAGGAGGAGGGGGAGATGCG GTCCGAGAGGACCGGCCAGTGTTACAACCAATTAAC
S19E/S216E	S19E Fw	CGTGCGCACGCCGCGCGAACGACGCTCGGCCTTGCGCGAACTGCTCC GCAAGCGCCGCCATAGGGATAACAGGGTAATCG
	S19E Rv	GCTGGCCAGCTCGCGTTGGCGGCGCTTGCGGAGCAGTTCGCGCAAGG CCGAGCGTCGTTCGCCAGTGTTACAACCAATTAACC
	S216E Fw	TACGCGAACGGCGGGAAAGCGGTCCTCTCGGACCGCAGAACCCCCTC CTCCTCCTCGTCATAGGGATAACAGGGTAATCG
	S216E Rv	GGTGGGAGAGCAACTCGGATGACGAGGAGGAGGAGGGGGTTCTGCG GTCCGAGAGGACCGGCCAGTGTTACAACCAATTAAC
K355Q 53-F	K355Q Fw	TTCGGCGAGGTCTGGCCGCTCGATCGCTATCGCGTGGTCCAGGTGGC GCGTAAGCACAGCGATAGGGATAACAGGGTAATCG
	K355Q Rv	CAGACCGTGAGCACCGTCTCGCTGTGCTTACGCGCCACCTGGACCAC GCGATAGCGATCGAGCGCCAGTGTTACAACCAATTAAC